Fish and Shellfish Immunology 92 (2019) 600–611

Contents lists available at ScienceDirect

Fish and Shellfish Immunology

journal homepage: www.elsevier.com/locate/fsi

Full length article

Grass carp ATG5 and ATG12 promote autophagy but down-regulate the transcriptional expression levels of *IFN-I* signaling pathway

Pengfei Chu[a,b], Libo He[a], Cheng Yang[a,b], Wencheng Zeng[c], Rong Huang[a], Lanjie Liao[a], Yongming Li[a], Zuoyan Zhu[a], Yaping Wang[a,d,*]

[a] State Key Laboratory of Freshwater Ecology and Biotechnology, Institute of Hydrobiology, Chinese Academy of Sciences, Wuhan, 430072, China
[b] University of Chinese Academy of Sciences, Beijing, 100049, China
[c] School of Urban Construction, Wuchang Shouyi University, Wuhan, 430072, China
[d] Innovative Academy of Seed Design, Chinese Academy of Sciences, Beijing, 100101, China

ARTICLE INFO

Keywords:
Autophagy
ATG5
ATG12
Grass carp (*Ctenopharyngodon idella*)
IFN-I
Innate immunity

ABSTRACT

Autophagy is an essential and conserved process that plays an important role in physiological homeostasis, adaptive response to stress and the immune response. Autophagy-related proteins (ATGs) are key components of the autophagic machinery. In the study, grass carp (*Ctenopharyngodon idella*) autophagy-related gene 5 (*ATG5*) and 12 (*ATG12*) were identified. In the gill and intestine, *ATG5* and *ATG12* were highly expressed, but after grass carp reovirus (GCRV) infection, they were decreased significantly. In *Ctenopharyngodon idella* kidney (CIK) cells, the sharp variation of *ATG5* and *ATG12* expression was observed after poly(I:C) infection. Subcellular localisation showed that ATG5 and ATG12 were evenly distributed in the cytoplasm and nucleus. However, the interaction between ATG5 and ATG12 was only found in cytoplasm in both 293T cells and CIK cells. In addition, the overexpression of ATG5 or ATG12 in 293T cells showed enhanced autophagy, and autophagic process was facilitated when ATG5 and ATG12 were simultaneously overexpressed. Dual-luciferase activity assay indicated that both ATG5 and ATG12 remarkably suppressed the promoter activity of *IRF3*, *IRF7*, and *IFN-I*. Further, ATG5 and ATG12 conjugate showed far stronger inhibitory affection on the expression of *IFN-I* than either ATG5 or ATG12 in response to poly(I:C) or GCRV infection. Taken together, the results demonstrate that grass carp ATG5 and ATG12 play an important role in innate immunity and autophagy.

1. Introduction

Autophagy is an essential and highly conserved process of degradation of intracellular components via the lysosomal machinery in response to nutrient starvation or other hostile environment [1–4]. This process is critical to maintaining physiological homeostasis, including cell growth, development, repair, and survival [5]. The classical regulation of autophagy induced by nutrient-deficiency is via mammalian target of rapamycin complex 1 (mTORC1) and AMP-activated protein kinase (AMPK) inhibiting and activating, respectively [1,4,6]. Under nutrient-rich conditions, mTORC1 is localised on the lysosomal surface via a Rag GTPase-dependent mechanism [7,8] and suppresses unc-51 like autophagy activating kinase 1 (ULK1) activity via phosphorylation [1]. On the contrary, under the condition of insufficient nutrition, mTORC1 activity is switched off and subsequently releases ULK1, initiating autophagy signaling [7,8]. Besides, autophagy is broadly implicated in the immune system [9,10].

Accumulating evidences indicate that autophagy plays an important role in both innate immunity and adaptive immunity. Pattern recognition receptors (PRRs) specifically recognise a series of highly conserved pathogenic microorganism structures to initiate immune system [11,12]. Autophagy interacts with PRRs in multiple pathways. First, PRRs recognise pathogen-associated molecular patterns (PAMPs) and damage-associated molecular patterns (DAMPs) to activate autophagy, subsequently, autophagy direct captures and degrades the invading intracellular microbes [13]. Second, autophagy can bring cytosolic PAMP molecules into the lumen, where they can bind the ligand recognition side of the PRRs, which is especially important for Toll-like receptors (TLR) members [14–16]. Third, nucleotide-binding domain and leucine-rich-repeat-containing (NLR) members, for example NLRC4 and NLRP4, could inhibit autophagy [17], on the other hand, autophagy factor, like ATG5, ATG9, can also inhibit retinoic acid-inducing

* Corresponding author. State Key Laboratory of Freshwater Ecology and Biotechnology, Institute of Hydrobiology, Chinese Academy of Sciences, Wuhan, 430072, China.
E-mail addresses: wangyp@ihb.ac.cn, wangyp.ihb@gmail.com (Y. Wang).

https://doi.org/10.1016/j.fsi.2019.06.014
Received 1 April 2019; Received in revised form 4 June 2019; Accepted 9 June 2019
Available online 25 June 2019

gene I-like receptors (RLR) signaling pathway [18,19]. In addition, autophagy also plays a vital impact on presenting major histocompatibility complex (MHC) class I and II elements for recognition by $CD4^+$ and $CD8^+$ T cells [20,21].

The autophagic formation and progress is controlled by autophagy-related proteins (ATGs) [6], 40 genes encoding ATG proteins have been identified so far, of which 15 core genes encoding ATG proteins in yeast (ATG1–ATG10, ATG12–ATG14, ATG16 and ATG18) are conserved in mammals, indicating autophagy is a conserved process [22]. In mammals, the core ATG proteins usually are classified into the following units according to their functions: the ULK complex, Beclin 1, Atg5–Atg12/Atg16L1 complex, and the microtubule-associated protein L chain 3s (LC3s) conjugate system [22,23]. ULK1 and 2 and Beclin 1 are thought to be the most upstream components in the autophagy pathway and initiate the downstream ATG conjugate cascade [24]. ATG16L1 and ATG12-ATG5 form a 2:2:2 complex, which specifically localises to the isolation membrane and functions as an“E3 enzyme” for LC3 lipidation [25,26]. Then, autophagosomes interact with endosomal and lysosomal organelles to mature into autolysosomes [6]. Thus, LC3 usually was used as a commonly marker for identification of autophagosomes. So far, little ATGs functional information in fish was reported. In the study, grass carp *ATG5* and *ATG12* were identified and the mRNA expression profiles were examined. Subcellular localisation and the interaction between ATG5 and ATG12 were analysed in *Ctenopharyngodon idella* kidney (CIK) and 293T cells. Besides, the affection of ATG5 and ATG12 on autophagic formation and progress was explored in 293T cells. In addition, the regulation of promoter activity of *IRF3*, *IRF7* and *IFN-I* by ATG5 and ATG12 was analysed. Furthermore, the negative regulation of ATG5 and ATG12 conjugate on *IFN-I* was detected. These findings will provide new insights for understanding the functions of *ATGs* gene in teleosts.

2. Materials and methods

2.1. Experimental fish and cells

The grass carp (weight, 40 ± 10 g; length, 15 ± 3 cm) used in the study were bred and cultivated in the GuanQiao Experimental Station, Institute of Hydrobiology, Chinese Academic of Sciences. The *Ctenopharyngodon idella* kidney (CIK) and ovary (CO) cells were bought from China Center for Type Culture Collection, incubating in 28 °C and 293T cells were a kind gift from Professor Wei Hu (Institute of Hydrobiology, Chinese Academy of Sciences), incubating in 37 °C. The two cell lines were maintained in low glucose Dulbecco's modified Eagle's medium (DMEM; Gibco, USA) supplemented with 10% fetal bovine serum in a humidified atmosphere with 5% CO_2 and 1% (v/v) penicillin-streptomycin.

2.2. GCRV challenge, poly(I:C) infection, and sampling

The GCRV preparation and GCRV challenge experiment were carried out as described previously [27]. Before GCRV challenge experiment, six healthy fish were selected and samples of the middle kidney, head kidney, blood, liver, brain, spleen, intestine, and gill were collected. After GCRV infection, the tissues were also randomly sampled from six infected fish for consecutive days.

In addition, to further explore the mechanism of *ATG5* and *ATG12* during the innate immune, the poly(I:C) (sigma, USA; 20 μg/ml) infection experiment in CIK cells seeded in six-well plates was performed and phosphate-buffered saline (PBS) was used as control groups. After poly(I:C) or PBS stimulation, cells from each group were harvested at 3, 8, 24, 36, and 48 h. All samples were homogenized in TRIzol reagent (Invitrogen, USA) and stored at −80 °C prior to RNA extraction.

2.3. Cloning the full-length cDNA of ATG5 and ATG12

Zebrafish (*Danio rerio*) *ATG5* and *ATG12* cDNA (Accession no. NM_001009914.2 and NM_001246200.1, respectively) were used to blast with draft genome of grass carp [28] to obtain the homologous sequences. Besides, 5′ and 3′ Full RACE Kit (TaKaRa, Japan) were used to obtain the untranslated regions (UTRs) of the *ATG5* and *ATG12* gene. The coding sequences (CDS) were amplified using PCR with primers within the 5′- and 3′-UTRs (Primers were listed in Table S1).

2.4. Sequence analysis

BLAST (https://blast.ncbi.nlm.nih.gov/Blast.cgi) was used to search for cDNA sequences of zebrafish. Amino acid sequences of ATG5 and ATG12 proteins were predicted using open reading frame (ORF) Finder (http://www.ncbi.nlm.nih.gov/projects/gorf/), and multiple sequence alignments were performed using ClustalW 2.1 (http://www.ebi.ac.uk/tools/clustalw2.1). Neighbour-joining (NJ) phylogenetic trees were constructed on the basis of the amino acid sequences by using MEGA 7.0 software (http://www.megasoftware.net/index.html) and the bootstrap values of the branches were obtained by testing the tree 1000 times.

2.5. The mRNA expression profiles of ATG5 and ATG12

To investigate the expression pattern of *ATG5* and *ATG12* in grass carp, the total RNA of samples and cDNA were obtained as described previously [29,30]. The samples from the middle kidney, head kidney, blood, liver, brain, spleen, intestine, and gill in healthy grass carp were used to detect the tissues distribution and samples from the gill, intestine, liver, and spleen from grass carps at different days after GCRV infection (days 0, 1, 2, 3, 4, 5, and 6) were used to examine their responses to GCRV infection. Besides, the mRNA expression levels of *ATG5* and *ATG12* in CIK cells were used to examine their responses to poly(I:C) stimulation. The housekeeping gene *β-actin* was used as a reference gene and the CFX96™ real-time PCR detection system (Bio-Rad, USA) was used to measure the mRNA expression levels of *ATG5* and *ATG12*. Primers for qRT-PCR were listed in Table S1. Relative expression levels of *ATG5* and *ATG12* were calculated using the $2^{-\triangle\triangle Ct}$ method [31].

2.6. Construction of plasmid vectors

To analyse the role of ATG5 and ATG12 in *IFN-I* signaling pathway, plasmid pHA-ATG5, pHA-ATG12, pIRF3pro-Luc, pIRF7pro-Luc, and pIFN-Ipro-Luc were constructed. The restriction sites *Eco*RI and *Kpn*I (NEB, USA) were introduced to construct pHA-ATG5 and pHA-ATG12 as described previously [32] (primers were listed in Table S1). The restriction sites *Kpn*I and *Xho*I (NEB, USA) were introduced to construct pIRF3pro-Luc, pIRF7pro-Luc, and pIFN-Ipro-Luc. The promoter region of *IRF3*, *IRF7* and *IFN-I* were cloned (primers were listed in Table S2), then digested and subcloned into *Kpn*I and *Xho*I sites of pGL3-Basic luciferase reporter vector (Promega, USA).

In addition, ATG5-pEGFP and ATG12-pEGFP vector were constructed to analyse the subcellular localisation of ATG5 and ATG12. The restriction sites *Eco*RI and *Kpn*I (NEB, USA) were used to subclone into pEGFP-N3 vector (Clontech, USA). Besides, pATG5-MN155 and pMC156-ATG12 were constructed to analyse the interaction of ATG5 with ATG12. The restriction sites *Hind*III and *Kpn*I were used to subclone into the pMN155, which contained the N-terminal of mNeptune (mNeptune aa 1–155, MN155) or pMC156 plasmids, which contained the C-terminal of mNeptune (mNeptune aa 156C-terminal, MC156), respectively (The plasmids pMN155 and pMC156 used in the study were a kind gift from Professor Zongqiang Cui, Wuhan Institute of Virology, Chinese Academy of Sciences and kept in our lab). Primers for constructing the above vectors were listed in Table S2.

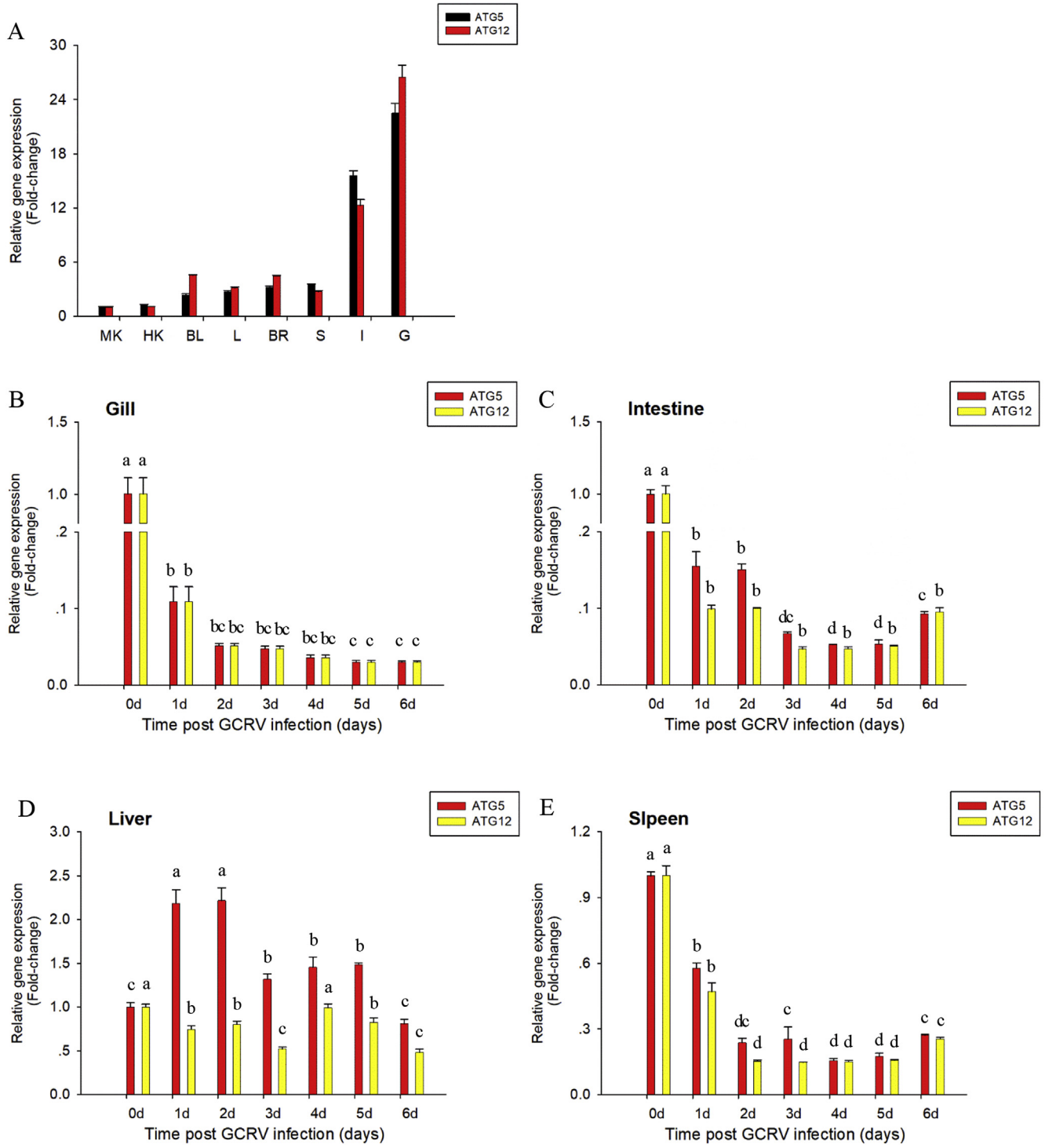

Fig. 1. Tissue distribution of *ATG5* and *ATG12* and expression pattern in response to GCRV infection. RNA extraction from grass carp tissues (middle kidney (MK), head kidney (HK), blood (BL), liver (L), brain (BR), spleen (S), intestine (I), and gill (G)) was subjected to qRT-PCR analysis. A. Relative mRNA expression levels of *ATG5* and *ATG12* were calculated on the basis of the ratio of gene expression in the different tissues relative to that in the middle kidney. The expression levels of *β-actin* were used as an internal control. B-E. The mRNA expression levels of *ATG5* and *ATG12* in the day 0 were set to 1 and *β-actin* was used as an internal control to normalize the relative mRNA expression levels of *ATG5* and *ATG12* in different tissues in response to GCRV infection. Error bars indicate standard deviation. The data (expressed as mean ± standard deviation) were analysed by one-way analysis of variance, followed by Dunnett's test for multiple comparisons using SPSS Statistics 19 software. Different hours labelled with different letters indicate statistically significant differences in mRNA levels ($p < 0.01$).

2.7. Subcellular localisation of ATG5 and ATG12

CIK cells were seeded evenly in six-well plates with glass bottom for 24 h to 70–80% confluence before transfection. Afterwards, ATGs-pEGFP or pEGFP (as control group) were transiently transfected into the CIK cells as the method described above. After 24 h transfection, cells were fixed with 4% paraformaldehyde, and stained with Hoechst 33342 (Beyotime, China). The cells were observed using the UltraVIEW VOX confocal system (PerkinElmer, Fremont, CA, USA) and a 63 × oil immersion objective lens.

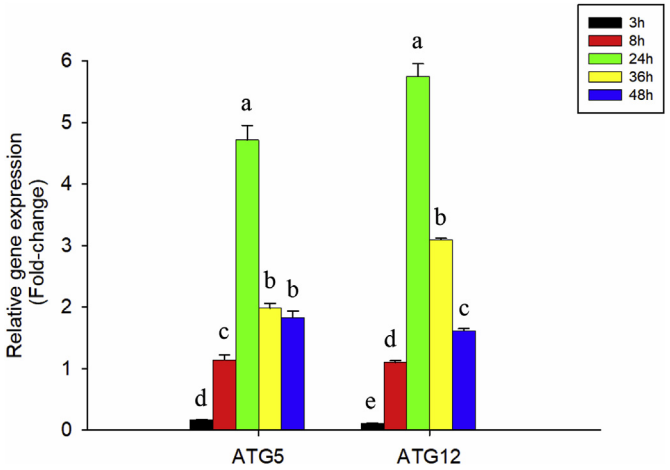

Fig. 2. Analysis of *ATG5* and *ATG12* gene expression after poly(I:C) stimulation. RNA extraction from each CIK cells group (3, 8, 24, 36, and 48 h after poly(I:C) stimulation) was subjected to qRT-PCR analysis. The mRNA expression levels of *ATG5* and *ATG12* in the PBS group at each point were set to 1 and *β-actin* was used as an internal control to normalize the relative expression levels of *ATG5* and *ATG12*. Error bars indicate standard deviation. The data (expressed as mean ± standard deviation) were analysed by one-way analysis of variance, followed by Dunnett's test for multiple comparisons using SPSS Statistics 19 software. Different hours labelled with different letters indicate statistically significant differences in mRNA levels ($p < 0.01$).

To further investigate the intracellular localisation of ATG5 and ATG12, pDsRed2-Mito vector (Clontech, USA) designed for fluorescent labeling of mitochondria, together with ATG5-pEGFP or ATG12-pEGFP, were transfected into CIK and 293T cells as the same transfection method described above. The cells were stained in the same way as the former groups.

2.8. Validation of the interaction between ATG5 and ATG12

In order to analyse whether grass carp ATG5 could interact with ATG12 in bimolecular fluorescence complementation (BiFC) system. Plasmids pATG5-MN155, which contained the N-terminal of mNeptune (mNeptune aa 1–155, MN155) alone or together with pMC156-ATG12, which contained the C-terminal of mNeptune (mNeptune aa 156C-terminal, MC156) were transfected into CIK and 293T cells as described above. After 24 h transfection, cells were fixed with 4% paraformaldehyde, and stained with Hoechst 33342 (Beyotime, China). The CIK cells were observed using the UltraVIEW VOX confocal system (PerkinElmer, Fremont, CA, USA) and a 63 × oil immersion objective lens.

2.9. The function of ATG5 and ATG12 in autophagy

To assess the role of ATG5 and ATG12 in autophagy induced by starvation, plasmids pHA-ATG5 and pHA-ATG12 were transiently transfected into the 293T cells. After 6 h transfection, the cells were incubated with adenovirus expressing GFP-LC3B fusion protein (Ad-GFP-LC3B, Beyotime, China). In addition, to further explore the role of ATG5 and ATG12 in the formation and progress of autophagy induced by starvation, 293T cells transfected with pHA-ATG5 and pHA-ATG12 were incubated with adenovirus expressing mCherry-GFP-LC3B fusion protein (Ad-mCherry-GFP-LC3B, Beyotime, China). After 36 h incubation without fetal bovine serum, the cells were fixed with 4% paraformaldehyde and stained with Hoechst 33342 (Beyotime, China). The 293T cells were observed using the UltraVIEW VOX confocal system (PerkinElmer, Fremont, CA, USA) and a 63 × oil immersion objective lens.

2.10. Dual-luciferase activity assays

In order to explore the role of ATG5 and ATG12 in *IRF-I* signaling pathway, 293T cells were seeded evenly in 24-well plate and incubated at 28 °C overnight. Subsequently, the cells were transfected with 250 ng of pIRF3pro-Luc or pIRF7pro-Luc or pIFN-Ipro-Luc, 250 ng of pHA-ATG5 or pHA-ATG12 or empty vector, and 2.5 ng of pRL-TK Renilla plasmid (Promega, USA) for 6 h. Then the medium was renewed by DMEM supplemented with 10% FBS and 1% penicillin-streptomycin, and incubating with poly(I:C) or PBS for 24 h. Cells were lysed by 200 ml of 1× Passive Lysis Buffer (Promega, USA) and luciferase activities were measured by using a Dual-Luciferase Reporter Assay System (Promega, USA).

2.11. ATG5 and ATG12 conjugate suppressed the expression levels of IFN-I signaling pathway

In order to further elucidate the role of ATG5 and ATG12 conjugate in the *IFN-I* signaling pathway, 2500 ng of pHA-ATG5, or pHA-ATG12, or pHA-ATG5 together with pHA-ATG12, or empty vector were transfected into CO cells seeded in 6-well plate as the method above (the transfection efficiency in CO cells is much higher than that of CIK cells). At 24 h post-transfection, cells were infected with poly(I:C) or GRV or PBS. At 36 h post-infection, total RNAs were extracted to examine the mRNA expression levels of *IRF3*, *IRF7*, and *IFN-I*.

2.12. Statistical analysis

The statistical results (expressed as mean ± standard deviation) were analysed by one-way analysis of variance, followed by Dunnett's test for multiple comparisons using SPSS Statistics 19 software. $p < 0.01$ was considered to be statistically significant. All experiments were repeated at least three times.

2.13. Key resources table

Resource	Source	Identifier
Cell Line		
293T	a kind gift from Professor Wei Hu (Institute of Hydrobiology, Chinese Academy of Sciences)	
CIK cells	China Center for Type Culture Collection, China	
CO cells	China Center for Type Culture Collection, China	
Chemical		
Hoechst 33342	Beyotime, China	
PBS	Gibco, America	
penicillin-streptomycin	YEASEN, China	
Protein Peptide		
ATG12	Cloning	
ATG5	Cloning	
GFP	Clontech, USA	
LC3B	Beyotime, China	

3. Results

3.1. Molecular characterisation and phylogenetic analysis of ATG5 and ATG12

The full length cDNA of *ATG5* (Genbank accession number: MK635464) is 1531 bp, containing a 5′ UTR of 23bp, an ORF of 828 bp and a 3′ UTR of 680 bp. The ORF encodes a predicted polypeptide of 275 amino acids. And the full length cDNA of *ATG12* (Genbank accession number: MK635465) is 553 bp long, containing a 5′ UTR of 31bp, an ORF of 363 bp and a 3’ UTR of 159 bp. The ORF encodes a predicted polypeptide of 120 amino acids (Fig. S1). Evolutionary relationship analysis based on the full-length amino acid sequences of

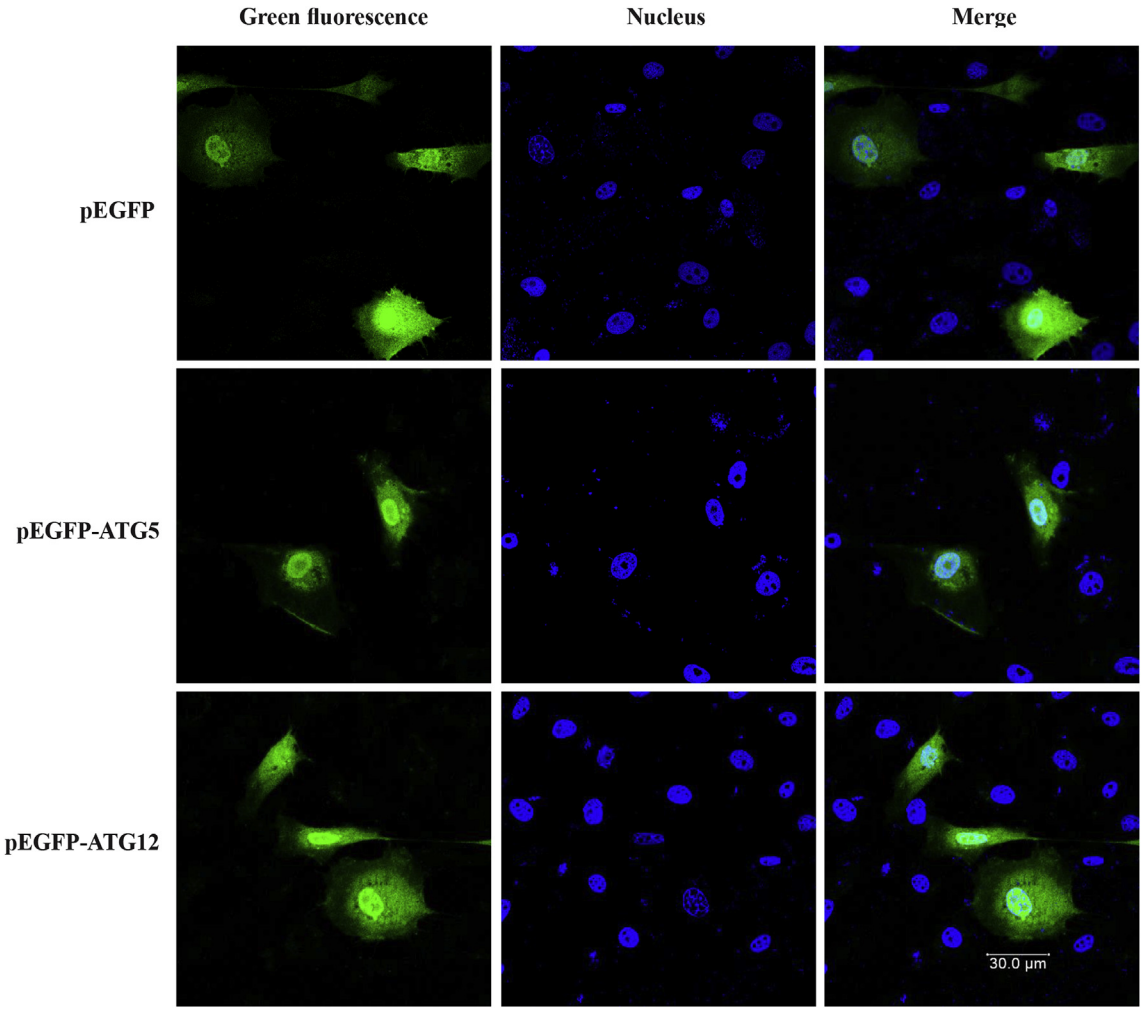

Fig. 3. Subcellular localisation of ATG5 and ATG12 in CIK cells. Cells were transfected with the plasmids ATG5-pEGFP or ATG12-pEGFP or pEGFP (as the control group) and fluorescence was observed at 24 h after transfection. Green fluorescence showed the distribution of GFP-tagged proteins, and blue fluorescence showed the nucleus stained with Hoechst 33342 under a 63 × oil immersion objective lens (scale bar, 30 μm). (For interpretation of the references to colour in this figure legend, the reader is referred to the Web version of this article.)

ATG5 and ATG12 with other species revealed that grass carp ATG5 and ATG12 were closely related to that of *C.carpio* (Fig. S2).

3.2. Tissue distribution of ATG5 and ATG12 in healthy grass carp

Eight tissues (middle kidney (MK), head kidney (HK), blood (BL), liver (L), brain (BR), spleen (S), intestine (I), and gill (G)) were sampled from healthy grass carps. The *ATG5* and *ATG12* mRNA expression levels in the tissues were examined by RT-qPCR. As shown in Fig. 1A, *ATG5* and *ATG12* were all mainly enriched in the gill and intestine, far more than that in the other tissues, and expressed the lowest in the middle kidney.

3.3. ATG5 and ATG12 mRNA expression levels following exogenous stimulants

To assess the role of *ATG5* and *ATG12* in innate immune, *ATG5* and *ATG12* mRNA expression levels in the gill, intestine, liver, and spleen from grass carp infected with GCRV were examined by RT-qPCR. As shown in Fig. 1B–E, in response to GCRV stimulation, *ATG5* and *ATG12* mRNA expression levels in the detected tissues were all decreased except *ATG5* in the liver, which increased rapidly in the first two day after GCRV infection.

In addition, *ATG5* and *ATG12* mRNA expression levels in CIK cells were detected in response to poly(I:C) stimulation. As shown in Fig. 2, *ATG5* and *ATG12* mRNA expression levels were significantly down-regulated in first 3 h after poly(I:C) stimulation, subsequently, dramatically increased and reached the peak at 24 h in response to poly(I:C) stimulation, after that it decreased at the late stage.

3.4. Subcellular localisation of ATG5 and ATG12

To investigate the subcellular localisation of ATG5 and ATG12, CIK cells were transfected with ATG5-pEGFP or ATG12-pEGFP, or pEGFP-N3 (as the control group) and then fluorescence was observed at 24 h after transfection. As shown in Fig. 3, both ATG5-pEGFP and ATG12-pEGFP were evenly distributed in the cytoplasm and nucleus, as the control group.

Further, in order to explore the mitochondria localisation of ATG5 and ATG12, pDsRed2-Mito (labeling of mitochondria) together with ATG5-pEGFP or ATG12-pEGFP, were transfected into CIK and 293T cells. As shown in Fig. 4A and B, the results indicated that ATG5 and ATG12 were partially located in the mitochondria.

3.5. The interaction of ATG5 with ATG12

In mammals, the conjunction of ATG5 and ATG12 plays a vital role in autophagic flux. In this study, the mNeptune-based BiFC system was

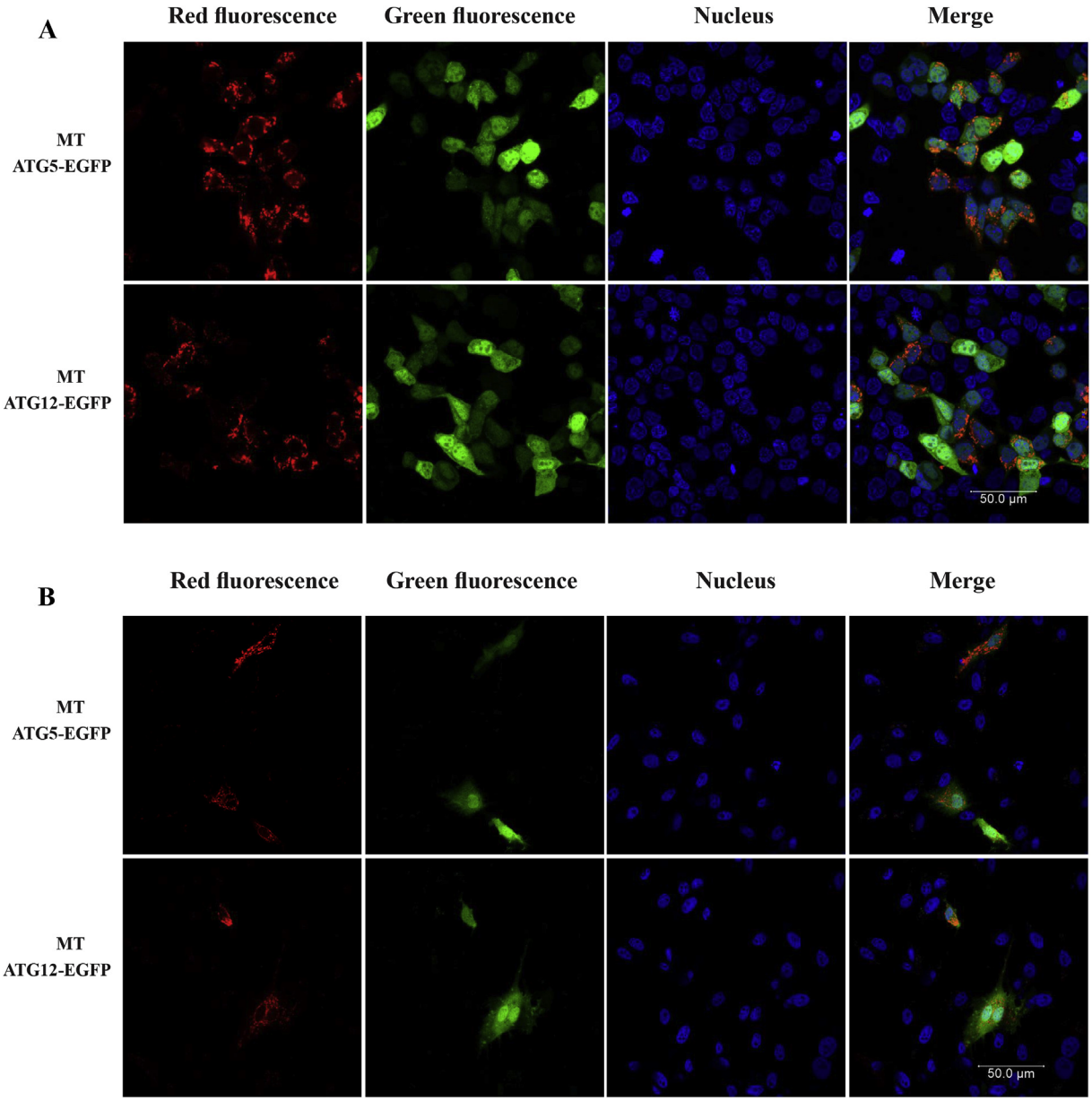

Fig. 4. The co-localisation of ATG5 and ATG12 with MT. Cells were co-transfected with pDsRed2-Mito and ATG5-pEGFP or ATG12-pEGFP, and fluorescence was observed at 24 h after transfection. Green fluorescence showed the distribution of ATG5 or ATG12 protein, Red fluorescence showed the distribution of MT, and blue fluorescence showed the nucleus stained with Hoechst 33342 under a 63 × oil immersion objective lens (scale bar, 50 μm). A. 293T cells, B. CIK cells. (For interpretation of the references to colour in this figure legend, the reader is referred to the Web version of this article.)

used to visualize the interaction of ATG5 with ATG12. As shown in Fig. 5A, the bright red mNeptune fluorescence signals were only occurred in the cytoplasm of CIK cells which were co-transfected with pATG5-MN155 and pMC156-ATG12, suggesting their conjunction was in the cytoplasm. However, the red signal was not observed when it came to the co-transfection with pATG5-MN155 and pMC156, or pMN155 and pMC156-ATG12. And the same results were also verified in 293T cells (Fig. 5B). Thus, the results further confirmed that ATG5 could interact with ATG12 in the cytoplasm.

3.6. ATG5 and ATG12 promoted autophagy

To corroborate the role of ATG5 and ATG12 in starvation-induced autophagy, 293T cells were transfected with pHA-ATG5 or pHA-ATG12 or pCMV-HA (as the control group) and incubated with adenovirus expressing GFP-LC3B fusion protein, which is the hallmark of autophagy induction [33,34]. As shown in Fig. 6, compared to the control, ATG5 and ATG12 detectably induced more GFP-LC3B puncta formation in the cytoplasm. The previous results in the study showed that the interaction between ATG5 and ATG12 was also in the cytoplasm. To further assess role of ATG5 and ATG12 conjugate, pHA-ATG5 and pHA-12 were co-transfected or transfected alone into 293T cells and incubated with adenovirus expressing mCherry-GFP-LC3B fusion protein. The LC3B protein localises in autophagosomes at the early stage of autophagy, emitting both mCherry (red) and GFP (green) signals. After fusion of autophagosomes with endosomal and lysosomal organelles to mature into autolysosomes, GFP fluorescence is quenched due to the low lysosomal pH resulting in mCherry-only labelled autolysosomes [35,36]. As shown in Fig. 7, in the control group, dispersedly yellow fluorescence (GFP and mCherry signals) were found in the cytoplasm and nucleus, representing diffuse LC3B protein. When transfection with pHA-ATG5 or pHA-12 alone, yellow puncta (merged by

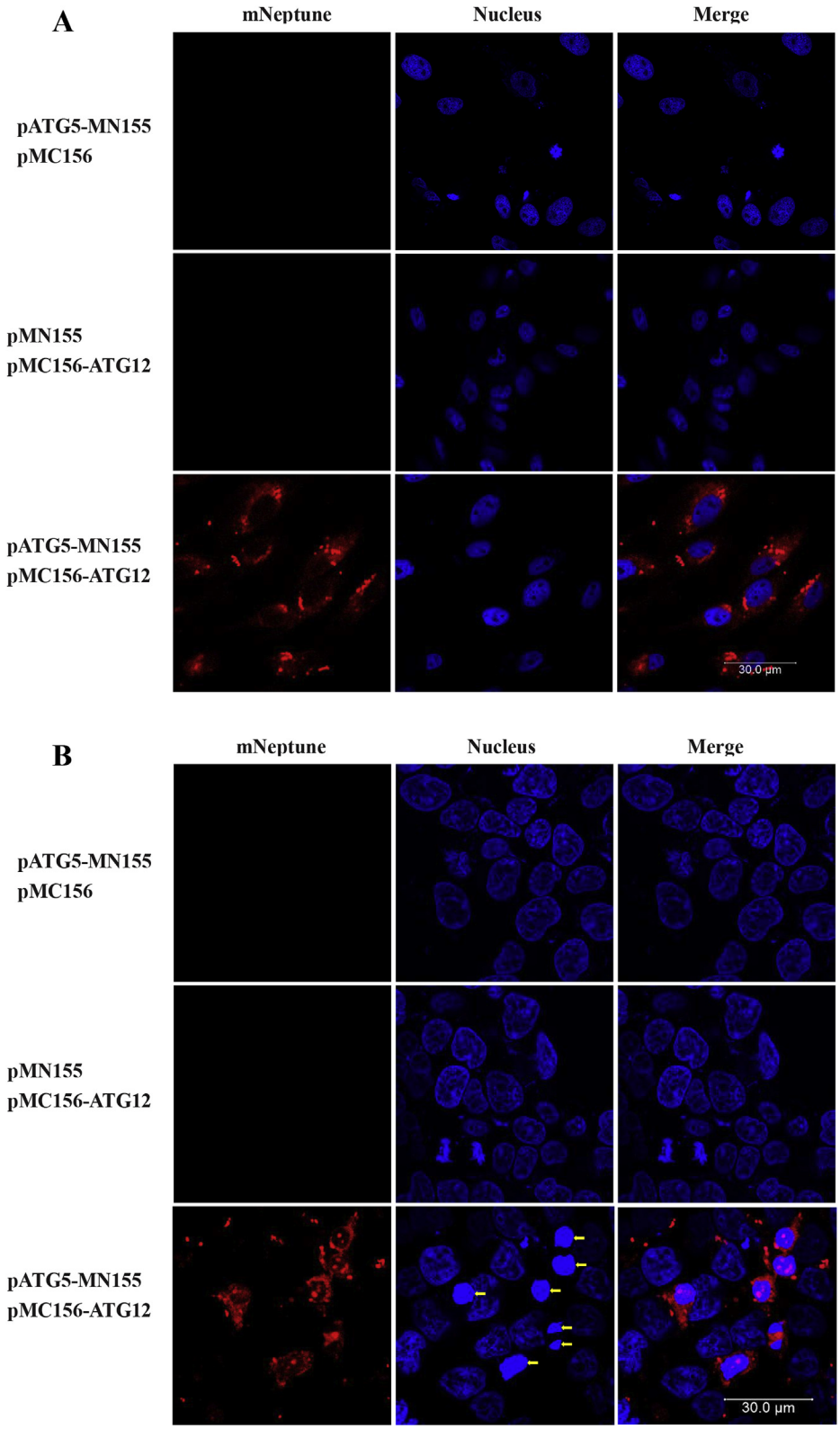

Fig. 5. The interaction of ATG5 with ATG12. Imaging of the protein-protein interaction was visualised by using far-red mNeptune-based BiFC in *vivo*. Plasmids pATG5-MN155 and pMC156-ATG12 were co-transfected into CIK and 293T cells. In the BiFC system, the fluorescence of the mNeptune channel was red, and the nucleus was stained with Hoechst 33342. The images were acquired using fluorescence microscopy and a 63 × oil immersion objective lens (scale bar, 30 μm). A. CIK cells, B. 293T cells. (For interpretation of the references to colour in this figure legend, the reader is referred to the Web version of this article.)

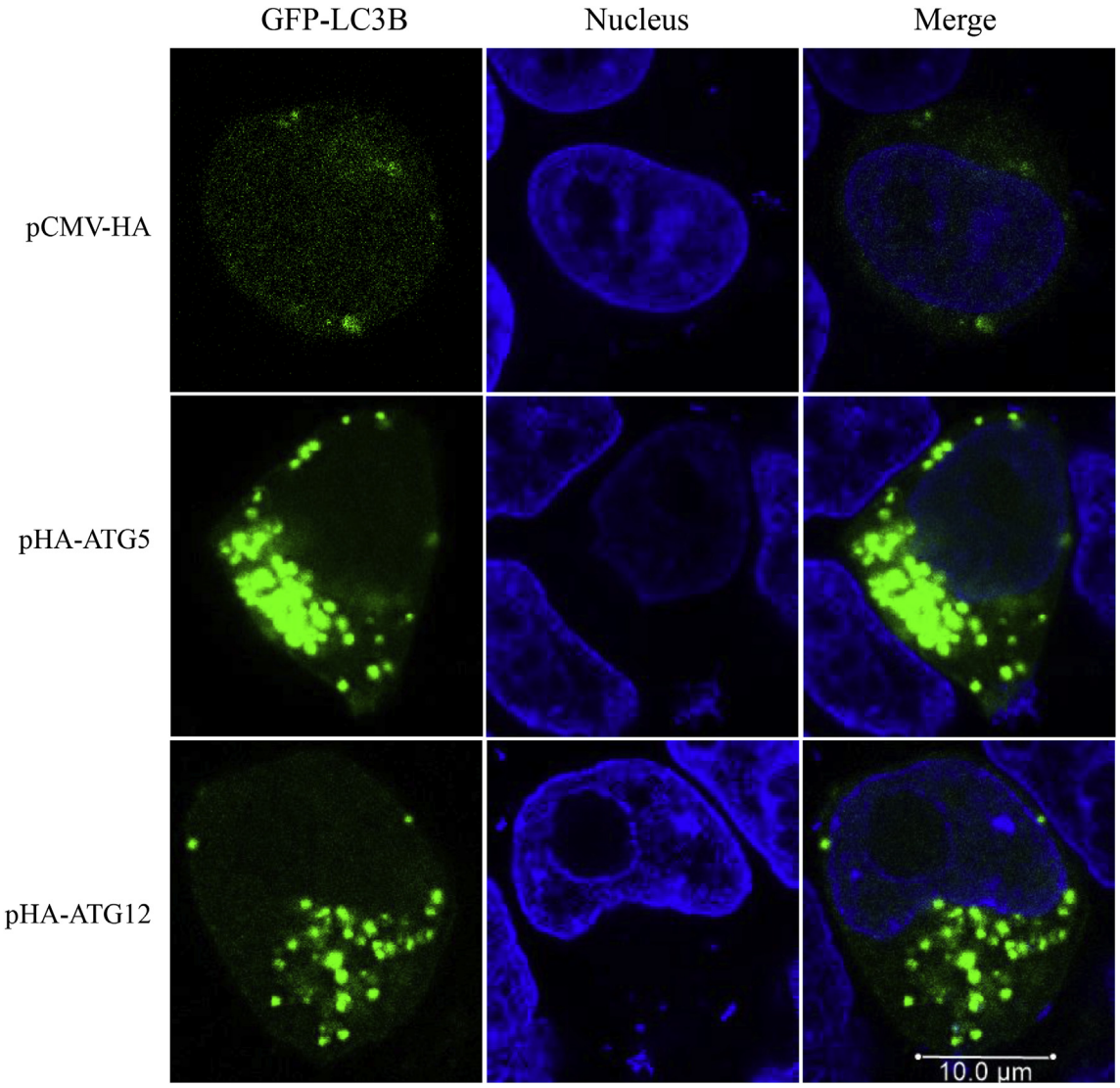

Fig. 6. ATG5 and ATG12 enhanced autophagy. Plasmids pHA-ATG5 or pHA-ATG12 had been transfected into 293T cells for 12 h and then cells were incubated with Ad-GFP-LC3B for another 36 h. After that, the cells were fixed with 4% paraformaldehyde and stained with Hoechst 33342. The images were acquired using fluorescence microscopy and a 63 × oil immersion objective lens (scale bar, 10 μm).

GFP puncta and mCherry puncta) were occurred, suggesting the formation of early autophagosomes. When co-transfection with pHA-ATG5 and pHA-ATG12, the pictures showed more of mCherry puncta than GFP signal, even in some vacuoles, there were only red fluorescence but no green fluorescence, indicating an increased autophagic flux.

3.7. ATG5 and ATG12 suppressed the transcriptional level of IFN-I signaling pathway

To analyse the role of grass carp ATG5 and ATG12 in *IFN-I* signaling pathway, the plasmids pHA-ATG5 or pHA-ATG12 or pCMV-HA (as the control group) were co-transfected into 293T cells with pIRF3pro-Luc, or pIRF7pro-Luc, or p IFN-Ipro-Luc and pRL-TK Renilla plasmid. As shown in Fig. 8, in normal condition, ATG5 repressed the promoter activity of *IRF3* and *IRF7*, but increased the promoter activity of *IFN-I*. ATG12 only increased the promoter activity of *IFN-I*, and had no effect on the *IRF3* and *IRF7*. However, after poly(I:C) stimulation, both ATG5 and ATG12 significantly suppressed the promoter activity of *IRF3*, *IRF7* and *IFN-I*.

3.8. ATG5 and ATG12 conjugate suppressed the expression levels of IFN-I signaling pathway

In order to further elucidate the role of ATG5 and ATG12 conjugate in the *IFN-I* signaling pathway, the plasmids pHA-ATG5, or pHA-ATG12, or pHA-ATG5 and pHA-ATG12 were transfected into CO cells. After exogenous stimulation, *IFN-I* signaling genes including *IRF3*, *IRF7*, and *IFN-I* were detected by qPCR. As shown in Fig. 9A, upon poly(I:C) stimulation, both ATG5 and ATG12 significantly down-regulated the expression of *IFN-I*. Besides, ATG5 and ATG12 conjugate showed far stronger ability to inhibit the expression of *IFN-I* than either ATG5 or ATG12. To our surprise, upon poly(I:C) stimulation, the expression levels of *IRF3* and *IRF7* in co-expressed ATG5 and ATG12 group were too low to be detected even though double amount of cNDA templates were tried (the results were not showed). Besides, the same results were also found when GCRV stimulation (Fig. 9B).

4. Discussion

The early reports on autophaic structures observed by electron microscopy could date back to the 1950s [37,38]. The early studies were

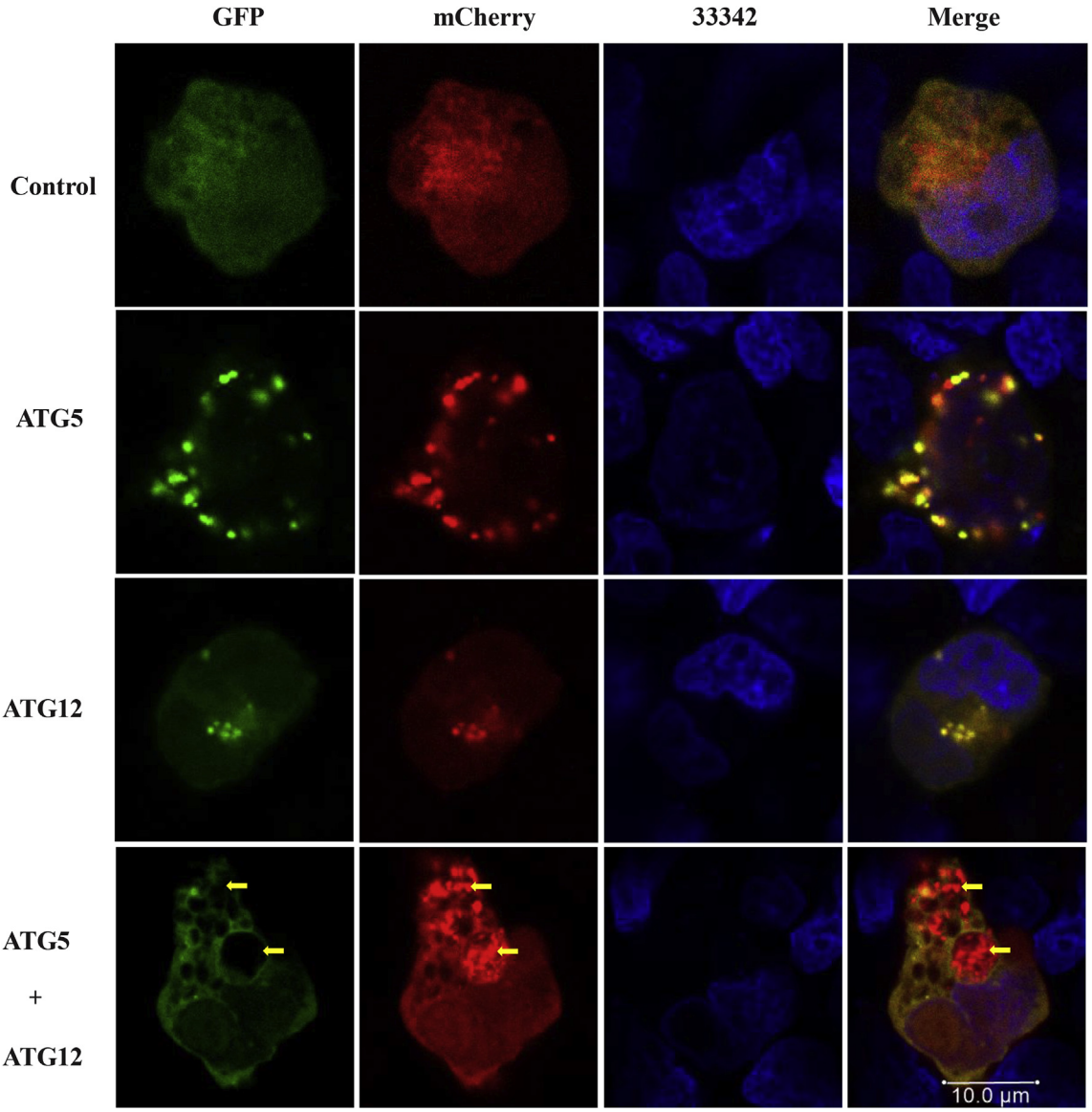

Fig. 7. The conjunction of ATG5 and ATG12 enhanced autophagic process. Plasmids pHA-ATG5 or pHA-ATG12 had been transfected into 293T cells alone or together for 12 h and then cells were incubated with Ad-mCherry-GFP-LC3B for another 36 h. After that, the cells were fixed with 4% paraformaldehyde and stained with Hoechst 33342. The images were acquired using fluorescence microscopy and a 63 × oil immersion objective lens (scale bar, 10 μm).

mainly restricted to its role in yeast about nonselective recycling of intracellular material to the lysosome upon starvation conditions [39,40]. With the discovery of yeast autophagy-related gene (ATG) in the 1990s and subsequent in-depth studies in various animal and cellular models, the molecular mechanism and the multiple functions of autophagy were gradually revealed [40,41]. Autophagic process usually goes through five stages: (1) signal initiation, (2) the formation of double-membrane phagophore (pre-autophagosome), (3) isolation of intracellular cargo, (4) autophagosome interact with lysosomal organelles to mature into autolysosomes, (5) cargo degradation. This process is controlled by the autophagy-related genes (ATGs) and additional factors [6,10]. Among ATGs, ATG5 and ATG12 are core and conserved mediators in autophagy in both yeast and mammals [22]. In the study, the grass carp *ATG5* and *ATG12* gene were clone and analysed. Phylogenetic tree analysis and multiple alignment of proteins showed that ATG5 and ATG12 were conserved in fishes, 93.6% and 92.9% with the homologues of other fishes, respectively, and ATG5 was even 65% homology with *Homo sapiens*, indicating autophagy is an evolutionally conserved process [1,22].

The expression pattern analysis of *ATG5* and *ATG12* in grass carp tissues showed that they were highly expressed in the gill and intestine, and low in the other tissues (Fig. 1A), indicated that the basic autophagy levels in the gill and intestine were far higher than that of other tissues, especially for the gill. That could be a beneficial evolution to adapt in the complex aquatic environment. Interestingly, except the liver, the mRNA expression levels of *ATG5* and *ATG12* were all decreased significantly during six days after GCRV infection (Fig. 1B–E). Previous study showed GCRV Virus rapidly proliferated in this stage and induced a strong immune response [34,42–44]. A growing evidences show virus infection and reproduction in *vivo* were related to ATG5/12-participated autophagy [45–47]. Viruses have evolved to utilize the autophagy machinery for promoting their infection and replication during long struggle against the immune system [48]. For example, Japanese encephalitis virus could utilize ATG5 and Beclin 1 to finish self-replication [49]. The nonstructural protein 4 (NSP4) colocalised with LC3 in the novel vesicular structures, the site was the nascent viral RNA replication [50]. However, whether GCRV replication is involved in autophagy needs further evidences.

In CIK cells, both ATG5 and ATG12 were evenly distributed in the cytoplasm and nucleus (Fig. 3). In mammals, the formation of double-

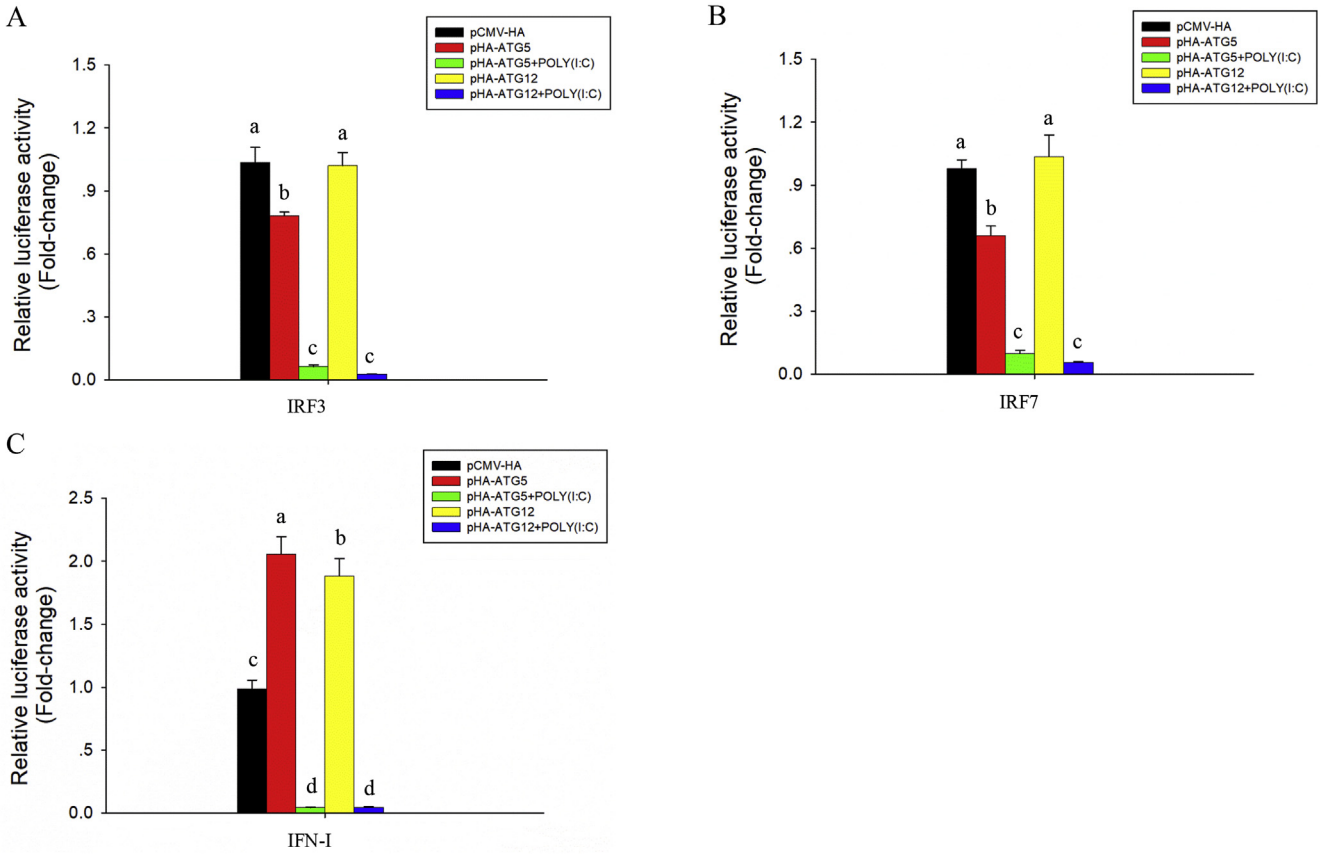

Fig. 8. The role of ATG5 and ATG12 in *IFN-I* signaling pathway. The regulative effect of ATG5 and ATG12 on the promoter activity of *IRF3*, *IRF7*, and *IFN-I* is monitored by dual-luciferase activity assays in 293T cells. Renilla luciferase activity was examined as the internal control and relative luciferase activity levels were expressed as fold increase of luciferase activity. Error bars indicate standard deviation. The data (expressed as mean ± standard deviation) were analysed by one-way analysis of variance, followed by Dunnett's test for multiple comparisons using SPSS Statistics 19 software. Different hours labelled with different letters indicate statistically significant differences in mRNA levels ($p < 0.01$).

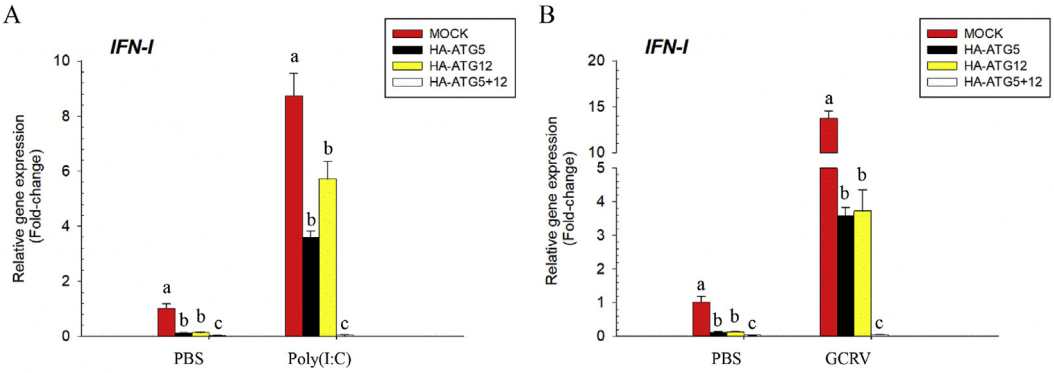

Fig. 9. ATG5 and ATG12 conjugate suppressed the expression levels of *IFN-I* signaling pathway. CO cells seeded in 6-well plate were transfected with 2500 ng of pHA-ATG5, or pHA-ATG12, or pHA-ATG5 together with pHA-ATG12, or empty vector, at 24 h post-transfection, cells were infected with poly(I:C) or GRV or PBS. At 36 h post-infection, total RNAs were extracted to examine the mRNA expression levels of *IRF3*, *IRF7*, and *IFN-I*. Error bars indicate standard deviation. The data (expressed as mean ± standard deviation) were analysed by one-way analysis of variance, followed by Dunnett's test for multiple comparisons using SPSS Statistics 19 software. Different hours labelled with different letters indicate statistically significant differences in mRNA levels ($p < 0.01$).

membrane phagophore always starts at contact sites between mitochondria (MT) and the endoplasmic reticulum (ER) [51]. In order to track the role of ATG5 and ATG12 in the original of autophagic process, ATG5 and ATG12 proteins were detected to partially co-locate with MT in 293T and CIK cells (Fig. 4A and B). As described previously, ATG5 and ATG12 were core proteins in the formation of autophagy [22,23], therefore, it is necessary to better understand the role of ATG5 and ATG12. In the study, the interaction between ATG5 and ATG12 was further visualised by BIFC system in both CIK and 293T cells (Fig. 5). Surprisingly, the bright red mNeptune fluorescence signals indicating their conjunction was only found in the cytoplasm, which was inconsistent with their intracellular localisation (Fig. 5). Besides, the nucleus was obviously condensed in 293T cells which occurred the conjunction of ATG5 and ATG12. We guess that ATG5 and ATG12 conjugate only occurred in the cytoplasm may be associated with the formation of autophagy. During autophagic process, LC3B fused with GFP usually was used as a commonly marker for identification of autophagosomes [33,34]. In 293T cells, the GFP puncta in overexpressed ATG5 or

ATG12 cells were far more than the control group under starving condition (Fig. 6), indicating either ATG5 or ATG12 overexpression could enhance the autophagy. Besides, the quenched GFP signaling in co-transfected ATG5 and ATG12 showed that the conjunction of ATG5 and ATG12 increased autophagic flux (Fig. 7), which further confirmed our hypothesis that the interaction of ATG5 with ATG12 are associated with the formation of autophagy.

In order to explore the role of ATG5 and ATG12 in innate immunity, the mRNA expression levels in CIK cells after poly(I:C) infection were detected. At the beginning (3 h after poly(I:C) infection), *ATG5* and *ATG12* expression were repressed, afterwards, they dramatically increased until reached to the peak at 24 h. In the late stage, they were declined (Fig. 2). The remarkable fluctuation of mRNA expression levels in response to poly(I:C) infection in CIK cells indicated *ATG5* and *ATG12* were involved in innate immunity. Dual-luciferase activity assays showed that the promoter activity of *IRF3*, *IRF7*, and *IFN-I* was all suppressed following poly(I:C) infection by overexpressing either ATG5 or ATG12 (Fig. 8), indicating ATG5 and ATG12 down-regulated the transcriptional level of *IFN-I* signaling pathway. In the study, previous results showed that ATG5 and ATG12 conjugate increased autophagic flux, which indicated ATG5 and ATG12 conjugate may play a vital role in biological function. However, whether ATG5 and ATG12 conjugate functioned significantly in immune system need further detect. Thus, the *IFN-I* signaling genes including *IRF3*, *IRF7*, and *IFN-I* were measured in overexpression ATG5 or ATG12 or ATG5 and ATG12 CO cells. After exogenous stimulation, ATG5 and ATG12 conjugate showed a much stronger inhibitory effect on the expression of *IFN-I* signaling genes (Fig. 9A and B). However, the mechanism of ATG5 and ATG12 conjugate regulate *IFN-I* signaling needs further study.

In conclusion, the grass carp *ATG5* and *ATG12* were cloned and analysed in the study. The conjunction of ATG5 and ATG12 in the cytoplasm strengthened the autophagic process. Besides, ATG5 and ATG12 involved in the innate immunity and down-regulated the transcriptional expression levels of *IFN-I* signaling pathway. The results provide new insights into understanding the functions of the *ATG5* and *ATG12* in teleosts.

Acknowledgments

This work was funded by the National Natural Science Foundation of China [grant number 31572614], the Strategic Pilot Science and Technology Projects (A) Category, Chinese Academy of Science [grant number XDA08030203], the State Key Laboratory of Freshwater Ecology and Biotechnology [grant number 2016FBZ02], the National Natural Science Foundation of China [grant number 31702332], and the Hubei Natural Science Foundation of China [grant number 2017CFB374].

Appendix A. Supplementary data

Supplementary data to this article can be found online at https://doi.org/10.1016/j.fsi.2019.06.014.

References

[1] J. Kim, M. Kundu, B. Viollet, K.L. Guan, AMPK and mTOR regulate autophagy through direct phosphorylation of Ulk1, Nat. Cell Biol. 13 (2011) 132–141.
[2] N. Mizushima, M. Komatsu, Autophagy: renovation of cells and tissues, Cell 147 (2011) 728–741.
[3] H.M. Shen, N. Mizushima, At the end of the autophagic road: an emerging understanding of lysosomal functions in autophagy, Trends Biochem. Sci. 39 (2) (2014) 61–71.
[4] J. Zhou, S.H. Tan, V. Nicolas, et al., Activation of lysosomal function in the course of autophagy via mTORC1 suppression and autophagosome-lysosome fusion, Cell Res. 23 (4) (2013) 508–523.
[5] B. Yordy, M.C. Tal, K. Hayashi, et al., Autophagy and selective deployment of Atg proteins in antiviral defense, Int. Immunol. 25 (1) (2013) 1–10.
[6] N. Mizushima, T. Yoshimori, Y. Ohsumi, The role of Atg proteins in autophagosome formation, Annu. Rev. Cell Dev. Biol. 27 (2011) 107–132.
[7] L. Bar-Peled, D.M. Sabatini, Regulation of mTORC1 by amino acids, Trends Cell Biol. 24 (7) (2014) 400–406.
[8] J.L. Jewell, R.C. Russell, K.L. Guan, Amino acid signalling upstream of mTOR, Nat. Rev. Mol. Cell Biol. 14 (3) (2013) 133–139.
[9] B. Levine, N. Mizushima, H.W. Virgin, Autophagy in immunity and inflammation, Nature 469 (2011) 323–335.
[10] Y. Ma, L. Galluzzi, L. Zitvogel, G. Kroemer, Autophagy and cellular immune responses, Immunity 39 (2013) 211–227.
[11] Y. Palti, Toll-like receptors in bony fish: from genomics to function, Dev. Comp. Immunol. 35 (12) (2011) 1263–1272.
[12] M.K. Purcell, K.D. Smith, L. Hood, J.R. Winton, J.C. Roach, Conservation of toll-like receptor signaling pathways in teleost fish, Comp. Biochem. Physiol. Genom. Proteonom. 1 (1) (2006) 77–88.
[13] D. Tang, R. Kang, C.B. Coyne, et al., PAMPs and DAMPs: signal 0s that spur autophagy and immunity, Immunol. Rev. 249 (2012) 158–175.
[14] H.K. Lee, J.M. Lund, B. Ramanathan, et al., Autophagy-dependent viral recognition by plasmacytoid dendritic cells, Science 315 (2007) 1398–1401.
[15] H.K. Lee, L.M. Mattei, B.E. Steinberg, et al., In vivo requirement for Atg5 in antigen presentation by dendritic cells, Immunity 32 (2010) 227–239.
[16] A. Chaturvedi, D. Dorward, S.K. Pierce, The B cell receptor governs the subcellular location of Toll-like receptor 9 leading to hyperresponses to DNAcontaining antigens, Immunity 28 (2008) 799–809.
[17] N. Jounai, K. Kobiyama, M. Shiina, et al., NLRP4 negatively regulates autophagic processes through an association with beclin1, J. Immunol. 186 (2011) 1646–1655.
[18] N. Jounai, F. Takeshita, K. Kobiyama, et al., The Atg5 Atg12 conjugate associates with innate antiviral immune responses, Proc. Natl. Acad. Sci. U.S.A. 104 (2007) 14050–14055.
[19] T. Saitoh, N. Fujita, T. Hayashi, et al., Atg9a controls dsDNA-driven dynamic translocation of STING and the innate immune response, Proc. Natl. Acad. Sci. U.S.A. 106 (2009) 20842–20846.
[20] L. Van Kaer, V.V. Parekh, J.L. Postoak, L. Wu, Role of autophagy in MHC class I-restricted antigen presentation, Mol. Immunol.. https://doi.org/10.1016/j.molimm.2017.10.021.
[21] C. Munz, Antigen processing for MHC class II presentation via autophagy, Front. Immunol. 3 (9) (2012).
[22] S.T. Shibutani, T. Saitoh, H. Nowag, et al., Autophagy and autophagy-related proteins in the immune system, Nat. Immunol. 16 (10) (2015) 1014–1024.
[23] V. Deretic, Autophagy: an emerging immunological paradigm, J. Immunol. 189 (1) (2012) 15–20.
[24] E. Itakura, N. Mizushima, Characterization of autophagosome formation site by a hierarchical analysis of mammalian Atg proteins, Autophagy 6 (2010) 764–776.
[25] N. Mizushima, A. Yamamoto, M. Hatano, et al., Dissection of autophagosome formation using Apg5-deficient mouse embryonic stem cells, J. Cell Biol. 152 (2001) 657–668.
[26] N. Fujita, T. Saitoh, S. Kageyama, et al., Differential involvement of Atg16L1 in Crohn disease and canonical autophagy: analysis of the organization of the Atg16L1 complex in fibroblasts, J. Biol. Chem. 284 (2009) 32602–32609.
[27] P. Chu, L. He, L. Xiong, et al., Molecular cloning, expression analysis and localization pattern of the MST family in grass carp (*Ctenopharyngodon idella*), Fish Shellfish Immunol. 76 (2018) 316–323.
[28] Y. Wang, Y. Lu, Y. Zhang, et al., The draft genome of the grass carp (*Ctenopharyngodon idellus*) provides insights into its evolution and vegetarian adaptation, Nat. Genet. 47 (6) (2015) 625–631.
[29] P. Chu, L. He, Y. Li, et al., Molecular cloning and functional characterisation of *NLRX1* in grass carp (*Ctenopharyngodon idella*), Fish Shellfish Immunol. 81 (2018) 276–283.
[30] D. Zhu, Y. Li, R. Huang, et al., Molecular characterization and functional activity of Prx1 in grass carp (Ctenopharyngodon idella), Fish Shellfish Immunol. 90 (2019) 395–403.
[31] K.J. Livak, T.D. Schmittgen, Analysis of relative gene expression data using realtime quantitative PCR and the $2^{-\triangle\triangle Ct}$ method, Methods 25 (4) (2001) 402–408.
[32] P. Chu, L. He, D. Zhu, et al., Identification, characterisation and preliminary functional analysis of *IRAK-M* in grass carp (*Ctenopharyngodon idella*), Fish Shellfish Immunol. 84 (2019) 312–321.
[33] K.M.J. Sparrer, S. Gableske, M.A. Zurenski, et al., TRIM23 mediates virus-induced autophagy via activation of TBK1, Nat. Microbiol. 2 (2017) 1543–1557.
[34] P. Chu, L. He, C. Yang, et al., Characterisation and function of *TRIM23* in grass carp (*Ctenopharyngodon idella*), Fish Shellfish Immunol. 88 (2019) 627–635.
[35] R.O. Walters, E. Arias, A. Diaz, et al., Sarcosine is uniquely modulated by aging and dietary restriction in rodents and humans, Cell Rep. 25 (3) (2018) 663–676.
[36] C. Zhang, J. Yan, Y. Xiao, et al., Inhibition of autophagic degradation process contributes to claudin-2 expression increase and epithelial tight junction dysfunction in TNF-alpha treated cell monolayers, Int. J. Mol. Sci. 18 (1) (2017) E157 pii.
[37] S.L. Clark Jr., Cellular differentiation in the kidneys of newborn mice studies with the electron microscope, J. Biophys. Biochem. Cytol. 3 (3) (1957) 349–362.
[38] A.B. Novikoff, The proximal tubule cell in experimental hydronephrosis, J. Biophys. Biochem. Cytol. 6 (1) (1959) 136–138.
[39] A. Zimmermann, K. Kainz, A. Andryushkova, et al., Autophagy: one more Nobel Prize for yeast, Microb. Cell 3 (12) (2016) 579–581.
[40] Z. Yin, C. Pascual, D.J. Klionsky, Autophagy: machinery and regulation, Microb. Cell 3 (12) (2016) 588–596.
[41] Y. Ohsumi, Historical landmarks of autophagy research, Cell Res. 24 (1) (2014) 9–23.
[42] L. He, A. Zhang, Y. Pei, et al., Differences in responses of grass carp to different types of grass carp reovirus (GCRV) and the mechanism of hemorrhage revealed by transcriptome sequencing, BMC Genomics 18 (1) (2017) 452.

[43] D. Zhu, R. Huang, P. Fu, et al., Investigating the role of BATF3 in grass carp (*Ctenopharyngodon idella*) immune modulation: a fundamental functional analysis, Int. J. Mol. Sci. 20 (7) (2019) 1687.
[44] D. Zhu, R. Huang, L. Chen, et al., Cloning and characterization of the LEF/TCF gene family in grass carp (Ctenopharyngodon idella) and their expression profiles in response to grass carp reovirus infection, Fish Shellfish Immunol. 86 (2019) 335–346.
[45] B.L. Schiøtz, N. Roos, A.L. Rishovd, T. Gjøen, Formation of autophagosomes and redistribution of LC3 upon in *vitro* infection with infectious salmon anemia virus, Virus Res. 151 (1) (2010) 104–107.
[46] C. Guévin, D. Manna, C. Bélanger, et al., Autophagy protein ATG5 interacts transiently with the hepatitis C virus RNA polymerase (NS5B) early during infection, Virology 405 (1) (2010) 1–7.
[47] A. Shroff, R. Sequeira, V. Patel, K. Reddy, Knockout of autophagy gene, ATG5 in mice vaginal cells abrogates cytokine response and pathogen clearance during vaginal infection of *Candida albicans*, Cell. Immunol. 324 (2018) 59–73.
[48] M. Desai, R. Fang, J. Sun, The role of autophagy in microbial infection and immunity, ImmunoTargets Ther. 4 (2015) 13–26.
[49] J.K. Li, J.J. Liang, C.L. Liao, Y.L. Lin, Autophagy is involved in the early step of Japanese encephalitis virus infection, Microb. Infect. 14 (2) (2012) 159–168.
[50] Z. Berkova, S.E. Crawford, G. Trugnan, et al., Rotavirus NSP4 induces a novel vesicular compartment regulated by calcium and associated with viroplasms, J. Virol. 80 (12) (2006) 6061–6071.
[51] M. Hamasaki, N. Furuta, A. Matsuda, et al., Autophagosomes form at ER-mitochondria contact sites, Nature 495 (2013) 389–393.